JOURNAL OF VIROLOGY, Dec. 1986, p. 1098–1106
0022-538X/86/121098-09$02.00/0

Vol. 60, No. 3

Simian Virus 40 Agnoprotein Facilitates Normal Nuclear Location of the Major Capsid Polypeptide and Cell-to-Cell Spread of Virus

JAMES RESNICK AND THOMAS SHENK*

Department of Molecular Biology, Princeton University, Princeton, New Jersey 08544

Received 9 June 1986/Accepted 5 September 1986

The simian virus 40 agnoprotein is a 61-amino-acid, highly basic polypeptide that is coded within the 5′ leader of late 16S mRNAs. To better understand agnoprotein function and to more effectively differentiate *cis*- from *trans*-acting effects of an agnogene mutation, we constructed a mutant virus that carries a single-base-pair substitution and fails to produce agnoprotein. *pm*1493 contains a T/A to A/T transversion at sequence position 335. This mutation converts the agnoprotein initiation codon from ATG to TTG, preventing synthesis of the protein. The mutant displays only a modest growth defect in CV-1P and AGMK cells and no defect in BSC-1 cells. Early-gene expression, DNA replication, synthesis of late viral products, and the kinetics of virion assembly all appear normal in *pm*1493-infected CV-1P cells. Immunofluorescent studies, however, indicate that localization of the major capsid polypeptide VP1 is different in mutant- than wild-type virus-infected cells. Furthermore, the lack of agnoprotein led to inefficient release of mature virus from the infected cell. Agnogene mutants could be severely compromised in their ability to propagate in monkeys given their reduced capacity for cell-to-cell spread.

The simian virus 40 (SV40) late transcription unit gives rise to a complex array of mRNAs. Transcription initiates at many sites within a 300-base-pair domain (5, 6, 11, 45). Primary transcripts are processed into 16S and 19S families of mRNAs by using several splice donor and acceptor sites (9, 25, 27, 46). Members of the 16S mRNA family are relatively homogeneous in their structure (see Fig. 1). Most have cap sites at sequence position 325, and all have undergone a splicing event which removes an intron located between sequence position 526 to 1463 (numbered according to Buchman et al. [4]). The 19S mRNA family is more heterogeneous (see Fig. 1). The cap sites of 19S mRNA map to a variety of positions, and the mature mRNAs can either be unspliced or spliced in several alternative patterns, the most common removing an intron located between positions 373 to 558.

The late mRNAs code for the three viral capsid polypeptides (VP1, VP2, and VP3) and for the agnoprotein (7, 10). The agnoprotein is coded within the 5′ leader region of most 16S mRNA family members (see Fig. 1). It is a highly basic, 71-amino-acid polypeptide. It is synthesized late after infection, accumulates in the perinuclear region, and binds to both single- and double-stranded DNA (19, 20, 38).

A wide variety of deletion and insertion mutations have been isolated which alter the agnogene (13, 33, 44, 48). These mutants are viable but display reduced growth rates compared with those of wild-type virus. They are *trans* complementable (35), suggesting their altered growth properties are due to the lack of a diffusible gene product. A variety of aberrations have been described for these mutants, including changes in the frequency with which various late cap sites and splice sites are used (9, 39, 40, 45, 46, 52). Altered mRNA structure, however, results from *cis*-acting effects of the mutations on the DNA template and probably does not involve altered or missing agnoprotein. Agnoprotein mutants have also been reported to assemble viral minichromosomes into virions at a slower rate than does wild-type virus (36). A role in capsid formation involving interaction with VP1 fits nicely with the finding that pseudorevertants of a VP1 mutant map in the agnoprotein coding region (28). Finally, transcriptional and translational regulatory functions have been postulated for the agnoprotein and its coding region (for a review, see reference 1). Evidence favoring the regulatory hypothesis includes premature transcriptional termination or pausing within the agnoprotein locus (26) at a sequence with structural similarity to bacterial attenuator elements in amino acid operons (16) and the finding that a *trans*-acting factor is encoded at the agnoprotein locus which influences late viral transcription (2). The regulatory model suggests that agnoprotein binds to the 5′ leader region of 16S mRNAs and influences its conformation. In its absence, transcription proceeds and 16S mRNAs assume a conformation which favors production of agnoprotein. In its presence, premature termination of transcription occurs and 16S mRNAs are translated to produce VP1 (1). A similar mechanism has been proposed to regulate translation of 19S mRNAs to produce VP2 and VP3 (1).

To better understand agnoprotein function and to differentiate effects of a mutation on the protein compared with its coding region, we constructed a mutant virus which carries a single-base-pair change and fails to produce agnoprotein. *pm*1493 contains a T/A base pair at position 335 in place of the normal A/T pair. This transversion converts the agnoprotein initiation codon from ATG to TTG, preventing synthesis of the protein. Early-gene expression, DNA replication, synthesis of late viral products, and capsid assembly appear normal in *pm*1493-infected monkey cells. Two effects of the mutation were observed. First, localization of VP1 capsid polypeptide was abnormal in *pm*1493-infected cells. Second, the lack of agnoprotein led to inefficient release of mature virus from infected cells.

* Corresponding author.

MATERIALS AND METHODS

Cells and viruses. CV-1P cells have been described (34), and BSC-1 cells were obtained from G. Khoury (National Institutes of Health). Both cell lines were maintained in medium containing 10% calf serum. Secondary African green monkey kidney cells were purchased from Flow Laboratories, Inc. (McLean, Va.) and maintained in medium supplemented with 10% fetal calf serum.

Wild-type SV40 (*wt*830) is a plaque-purified derivative of the SVS strain (50). *dl*1470 lacks 255 base pairs, which includes the N-terminal domain of the agnoprotein (8). *in*1494 was generated by repairing the termini of *Hpa*II-cleaved pSV3 DNA with the Klenow fragment of *Escherichia coli* DNA polymerase I, followed by recircularization of the blunt-ended molecule with T4 DNA ligase, excision of the SV40 genome from the plasmid, and transfection of CV-1P cells. *in*1494 carries a 2-base-pair insert between sequence positions 346 and 347. *pm*1493 contains an A to T transversion at sequence position 335 within the translational initiation codon (ATG to TTG) of the agnoprotein. The mutation was constructed into *wt*830 by oligonucleotide-directed mutagenesis. Mutagenesis was performed on a segment of SV40 DNA (sequence positions 215 to 348) which was inserted into M13mp10 between *Sal*I and *Sma*I cleavage sites. The orientation of the insert was such that single-stranded M13 recombinant DNA carried SV40 early-strand sequences. The oligonucleotide 5′-TTCAGGCCTT-GGTGCT-3′ (transversion is underscored) was synthesized by a modification of the phosphite-coupling method (29), annealed to the single-stranded M13 recombinant DNA, and extended as described by Zoller and Smith (55). Extended products were transformed directly into JM101 without enrichment for covalently closed circles. Since DNAs bearing the desired mutations would lack the single *Nco*I cleavage site present in the M13 clone, the mutated replicative form was enriched from a large pool of plaques by cleavage with *Nco*I followed by retransformation into JM101. After three cycles of enrichment, individual mutant clones were identified on the basis of having acquired a *Stu*I cleavage site at the position of the mutation. The mutation was then confirmed by DNA sequence analysis (30). A mutated SV40 segment was removed from M13 replicative-form DNA by cleavage with *Kpn*I and *Hpa*II and substituted for the corresponding wild-type DNA segment in a recombinant pBR322 carrying the entire SV40 chromosome (pBR322 and SV40 joined through their unique *Bam*HI cleavage sites). The mutated SV40 genome was then excised from pBR322 by cleavage with *Bam*HI and introduced into CV-1P cells by the DEAE-dextran transfection procedure (34). Mutant virus was plaque purified twice, and the presence of the mutation was confirmed by cleavage with *Stu*I and DNA sequencing.

DNA replication assay. CV-1P cells were harvested at various times after infection at a multiplicity of 4 PFU per cell. SV40 DNA was isolated by the procedure of Hirt (17), digested with *Hin*dIII, and subjected to Southern-type DNA blot analysis (47). SV40 DNA labeled with ^{32}P by nick translation (42) was used as probe.

RNA preparation and analysis. To monitor steady-state RNA levels, cytoplasmic, poly(A)$^+$ RNA was prepared (31) from CV-1P cells at various times after infection at a multiplicity of 3 PFU per cell. For Northern-type RNA blot analysis, RNA (for analysis of early mRNA, 2.5 μg; for late mRNA, 0.2 μg) was subjected to electrophoresis in formaldehyde-containing agarose gels (41) and blotted to nitrocellulose (3). Probe DNAs specific for early region mRNAs (pBR322 containing SV40 nucleotides 2771 to 3719) or late region mRNAs (pB322 containing SV40 nucleotides 874 to 2141) were labeled with ^{32}P by nick translation. 5′-S1 endonuclease analysis (53) used probe DNA fragments specific for wild type or mutant. The probes were end labeled with ^{32}P at the unique SV40 *Hpa*II site (sequence position 348) and extended to the unique *Bgl*I site (sequence position 1). Probe DNA strands were separated by electrophoresis on a 4% polyacrylamide gel as described by Szalay et al. (49).

Transcription rates were measured in isolated nuclei essentially as described by Groudine et al. (12) and Hofer and Darnell (18). Nuclei were prepared from CV-1P cells at 36 h after infection at a multiplicity of 4 PFU per cell. The nuclei were incubated for 15 min at 30°C in the presence of [α-^{32}P]UTP (1,250 mCi/ml, 410 Ci/mmol), and nuclear RNA was isolated, degraded by treatment with 0.2 N NaOH for 10 min at 4°C, and hybridized to single-stranded probe DNAs bound to nitrocellulose filters (100 μg of genome equivalents per filter) by the method of McKnight and Palmiter (32). The M13 probe DNAs contained SV40 sequences extending from sequence positions 294 to 500 and 874 to 2141.

Protein analysis. CV-1P cells were infected with SV40 at a multiplicity of 4 PFU per cell. Cells to be labeled with [^{14}C]arginine (100 μCi/ml, 350 mCi/mmol) were first maintained in medium lacking arginine for 90 min. Cells were labeled for brief periods with [^{35}S]methionine (100 μCi/ml, 1,100 Ci/mmol) in medium lacking methionine. When the labeling period was long (20 h) cells received medium containing 7.5 μg of methionine per ml. Immunoprecipitations used a serum prepared with an agnoprotein-specific peptide (38) obtained from G. Jay (National Institutes of Health), a monoclonal antibody (mAB594) specific for VP1 provided by E. Harlow (Cold Spring Harbor Laboratory), or a monoclonal antibody (PAB416 [14]) specific for large T antigen also provided by E. Harlow. Preparation of cellular extracts and immunoprecipitations was according to procedures described by Tegtmeyer et al. (51), and electrophoresis was performed as described by Laemmli (24), with the exception of agnoprotein immunoprecipitations which were analyzed in the phosphate-urea electrophoresis system described by Shapiro et al. (43).

For immunofluorescent analyses, CV-1P cells were seeded onto cover slips and infected at a multiplicity of 1 PFU per cell. At various times after infection, cover slips were washed in phosphate-buffered saline at 4°C, fixed for 10 min at the same temperature in 50% acetone–50% methanol, and incubated for 30 min at 37°C with monoclonal antibody to VP1. Cover slips were washed with phosphate-buffered saline and then incubated for 30 min at 37°C with fluorescein-conjugated goat anti-mouse antibody (Cooper Biomedical, Inc., West Chester, Pa.).

Cell fractionations were done by a modification (23) of the double-detergent method of Weinberg and Penman (54). The cytoplasmic fraction was obtained by lysis of cells in hypotonic buffer containing 0.5% Nonidet P-40 followed by centrifugation to pellet nuclei. Pelleted nuclei were suspended in buffer containing 1% Nonidet P-40 and 0.5% sodium deoxycholate. Nuclei were again pelleted by centrifugation to generate the nuclear fraction. The supernatant was the outer nuclear membrane fraction.

Virus assembly. At 36 h after infection of CV-1P cells at a multiplicity of 4 PFU per cell, cells were labeled for 15 min with [^3H]thymidine (130 μCi/ml, 55 Ci/mmol); cell monolayers were then washed and subjected to chase periods for various times in medium supplemented with 2 μg of unlabeled thymidine per ml. SV40 nucleoproteins were extracted

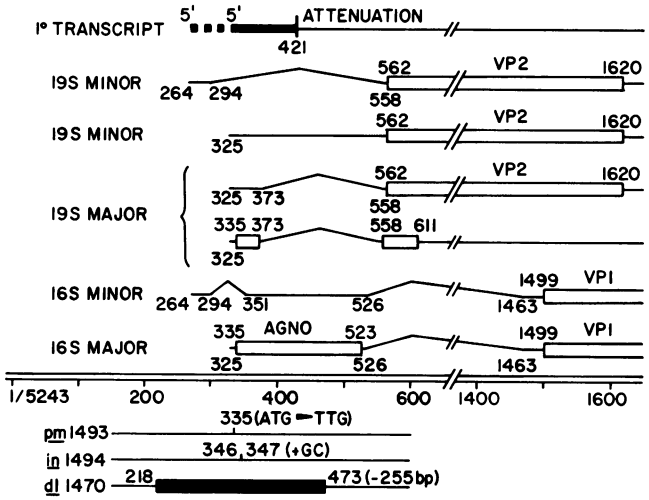

FIG. 1. Physical map of 5′ domains of SV40 late mRNAs, coding regions, and agnogene mutations. The double line positions the map in terms of the SV40 nucleotide sequence. mRNAs are designated by lines, introns by caret symbols, and coding regions by open rectangles. Numbers below RNA molecules refer to landmarks in the RNA, numbers above the molecules designate coding boundaries. The primary transcript at the top of the diagram indicates the site at which transcriptional attenuation occurs. Key mutations are diagrammed at the bottom of the figure. Nucleotide sequence numbers designate the site of a single-base-pair (bp) substitution or the base pairs which bracket either insertion or deletion mutations.

and analyzed by velocity sedimentation in sucrose gradients as described by Ng et al. (36).

RESULTS

Construction and growth of *pm*1493. A substantial number of deletion mutants, such as *dl*1470 (Fig. 1), which prevent synthesis of the agnoprotein have been isolated and characterized. As mentioned above, these deletion mutations often cause multiple effects, including alteration of late mRNA 5′ ends and splice site utilization. Two mutant viruses carrying more subtle alterations and expected to display phenotypes specific to the loss of agnoprotein were produced. *pm*1493 carries a single-base-pair substitution at sequence position 335, converting the agnoprotein initiator ATG to TTG, and *in*1494 contains a 2-base-pair insertion between sequence position 346 and 347 which introduces a frame shift into the agnoprotein coding region (Fig. 1).

The mutations were initially constructed into viral chromosomes carried in pBR322. To evaluate the growth potential of the mutant, SV40 sequences were excised from wild-type (pSV3), substitution (pSV335), and insertion (pSV346) variant-containing plasmids and used to transfect CV-1P cells (Table 1). Both variant DNAs gave rise to somewhat fewer and considerably smaller plaques than an equivalent portion of wild-type DNA. Curiously, however, the variants produced plaques of quite different sizes. The plaque sizes of the insertion mutant were substantially smaller than were those of the substitution mutant. We believe the plaque-size phenotype of the insertion mutant is the sum of two effects. First, as expected, functional agnoprotein is not made. Second, the N-terminal domain of the agnoprotein is likely appended to VP2 since the 2-base-pair insertion shifts the agnoprotein reading frame into the VP2 frame with no intervening termination codon in the most prevalent, spliced 19S mRNA family members. Thus, the phenotype of the insertion mutant is probably due in part to production of altered VP2. Consistent with this proposal, a double mutant (pSV346/335) exhibited the same phenotype as the less defective substitution mutant (Table 1). In this case, the frame-shifted agnoprotein domain was not translated, and the agnoprotein segment could not be appended to VP2. This interpretation also fits well with the finding of Nomura et al. (37) that their independently constructed 2-base-pair insertion mutant spontaneously gave rise to partial revertants by acquiring second-site mutations which could prevent an agnoprotein-VP2 fusion.

To focus specifically on the phenotype resulting from loss of agnoprotein, the insertion mutant was set aside and the substitution variant (pSV335) chosen for study. The mutated domain in pSV335 (sequence positions 215 to 348) was replaced with wild-type sequences, generating pSV335R. As expected, the revertant DNA produced the same number and size of plaques as did wild-type DNA (Table 1), proving the pSV335 phenotype was caused by a change in this small region. The mutant segment was sequenced and contained only the A to T transversion at position 335. Virus was then isolated from a pSV335-generated plaque and grown into a virus stock designated *pm*1493.

The inability of *pm*1493 to produce agnoprotein was next confirmed. *dl*1470, which lacks the coding region (Fig. 1) and could not produce agnoprotein, was included as a control. Cells were infected with mutant or wild-type viruses and labeled with [^{14}C]arginine for 1.5 h at various times after infection. Electrophoretic analysis of either immunoprecipitated agnoprotein (Fig. 2A) or total cell extracts (Fig. 2B) clearly demonstrated that agnoprotein was produced in wild-type but not mutant virus-infected cells. Further, agnoprotein was not produced at detectable levels in *wt*830-infected cells until relatively late (36 h) after infection, as has been reported previously (20).

Both agnoprotein mutants generated yields reduced by a factor of 3 or 4 compared with those of wild-type virus in CV-1P (Fig. 3A) or secondary AGMK (Fig. 3C) cells. No growth defect was observed in BSC-1 cells (Fig. 3B).

We concluded that both *pm*1493 and *dl*1470 fail to produce the agnoprotein and, as a result, display modest growth defects in some (CV-1P and AGMK) but not other (BSC-1) monkey cells.

Early- and late-gene expression appeared normal in the absence of agnoprotein. No difference was observed in steady-state levels of early mRNAs which accumulated in *pm*1493 or *dl*1470 compared with those of wild-type (*wt*830) virus-infected CV-1P cells at any time tested (Fig. 4A). Large T-antigen levels were also normal (Fig. 4B), and DNA replication proceeded normally in the absence of agnoprotein (Fig. 4C).

TABLE 1. DNA infectivity on CV-1P cells[a]

Plasmid	Virus	DNA PFU/μg ($\times 10^3$)	Plaque diameter (mm)
pSV3	*wt*830	7.6	5.0
pSV335	*pm*1493	4.0	1.0
pSV335R		7.6	5.0
pSV346	*in*1494	2.0	Pinpoint
pSV346/335	*in*1494/93	3.4	1.0

[a] Viral DNA was excised from plasmid sequences by cleavage with *Bam*HI. Plaque numbers and average diameters were determined on day 14 after the viral DNA was introduced into CV-1P cells by the DEAE-dextran transfection procedure.

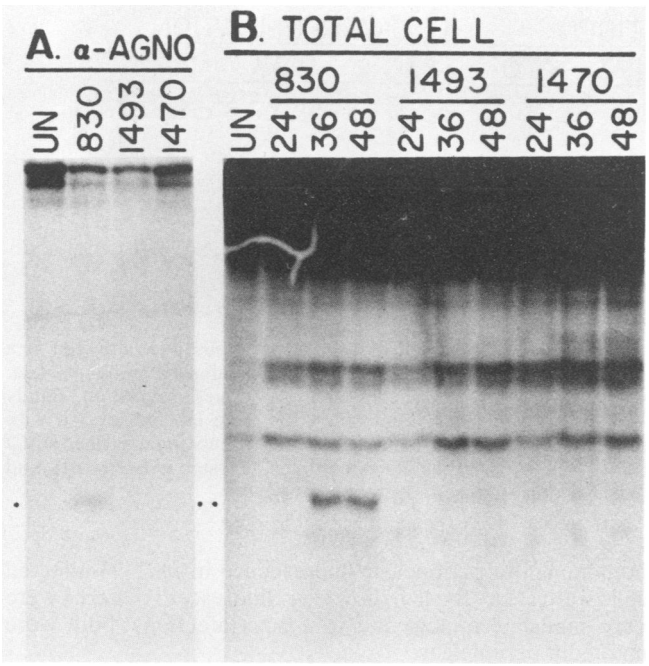

FIG. 2. Analysis of the agnoprotein synthesized in CV-1P cells after infection with mutant or wild-type viruses. Cells were labeled for 1.5 h with [^{14}C]arginine at various times after infection at a multiplicity of 4 PFU per cell. (A) Analysis of agnoprotein labeled at 48 h after infection and subjected to immunoprecipitation with a monospecific polyclonal antibody. (B) Analysis of total cell extracts labeled at the times indicated above each lane. Lanes UN, uninfected. The positions of bands corresponding to agnoprotein are marked by dots.

Late-gene expression was also monitored. Since agnoprotein has been postulated to play a role in attenuation of the late transcription unit (1, 16), we carefully monitored transcription rates upstream and downstream of the premature termination or pausing site identified by Laub et al. (26). The analysis was performed at 36 h after infection when agnoprotein was actively synthesized (Fig. 2). Transcription rates were assayed by using region-specific DNA fragments to probe ^{32}P-labeled RNA produced during runoff of transcribing polymerase in nuclei isolated from cells late after infection (Table 2). Premature termination or pausing was pronounced. However, little difference was evident in its frequency in the presence (*wt*830) or absence (*pm*1493) of agnoprotein. Similar results were obtained for an assay performed at 48 h after infection.

Hay and Aloni (15) reported that mutant Δ79 (identical to *in*1494) failed to accumulate in isolated nuclei a 94-nucleotide RNA which is normally generated by premature termination. Since this mutant does not encode functional agnoprotein, the result suggested a requirement for it in attenuation. Our data do not support such a role for agnoprotein. It is difficult to reconcile the conflicting results except to note that different mutants were evaluated by quite different assays.

Although no difference was evident at 24 h after infection, a modest increase (1.5- to 2-fold) in steady-state levels of late mRNAs was consistently observed in mutant compared with wild-type virus-infected cells (Fig. 5). We believe this modest effect is real because early mRNA levels were monitored from the same RNA preparations (Fig. 4A) and provide an internal control. Late mRNA 5′ ends were mapped by 5′-S1 analysis (Fig. 6). As has been well documented, a wide variety of ends were evident, with major species mapping to sequence positions 325, 264, and about 95. *wt*830 and *pm*1493 encode late mRNAs with identical cap sites. *dl*1470, which lacks the normal 325 and 264 start sites, has previously been demonstrated to use upstream cap sites (9) and was not reanalyzed here. *in*1494, which contains a 2-base-pair insert within the agnoprotein coding region (Fig. 1), was tested and found to favor upstream cap sites at the expense of the 325 start site. Since *pm*1493 fails to produce agnoprotein but uses normal 5′ ends, we concluded that cap site selection must be altered in response to a *cis*-acting alteration (2-base-pair insert) in the *in*1494 DNA template. Agnoprotein does not influence late mRNA cap site selection.

Finally, late polypeptide synthesis was monitored. No difference in the rate of VP1 synthesis was evident when the polypeptide was immunoprecipitated from extracts of mutant or wild-type virus-infected cells that were labeled briefly with [^{35}S]methionine at various points during the late phase of the infectious cycle (Fig. 7A). VP1, VP2, and VP3 accumulation also appeared normal in nuclear extracts of mutant-infected cells labeled briefly with [^{14}C]arginine (Fig. 7B). Agnoprotein does not detectably influence the rate of late polypeptide synthesis.

Virus maturation was not detectably perturbed in the absence of agnoprotein. Agnoprotein has been proposed to expedite virus assembly since several agnogene deletion mutants were found to convert 75S chromatin into 220S virions more slowly than did wild-type virus (36). To explore this possibility, CV-1P cells were labeled with [^{3}H]thymidine for 15 min at 36 h after infection and then chased in the presence of excess unlabeled thymidine for either 2 or 8 h. After the chase period, cell extracts were prepared and SV40 nucleoprotein complexes were displayed on sucrose gradients (Fig. 8). Agnoprotein did not detectably influence the rate at which slower-sedimenting material was converted to species which cosedimented with 220S virions.

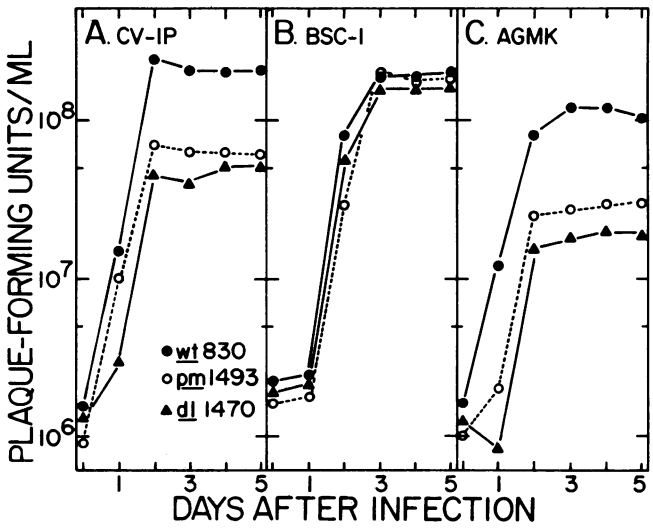

FIG. 3. Growth kinetics of mutant and wild-type viruses in various cell types. CV-1P (A), BSC-1 (B), or AGMK (C) cells were infected at a multiplicity of 4 PFU per cell. Cultures were harvested, subjected to three freeze-thaw cycles, and the virus yield determined at the times indicated by plaque assay on CV-1P cells.

FIG. 4. Characterization of early events in mutant and wild-type virus-infected cells. For all assays, CV-1P cells were infected at a multiplicity of 4 PFU per cell, and samples were analyzed at the times indicated directly above each lane. (A) Blot analysis of early mRNAs. Cytoplasmic, poly(A)$^+$ mRNAs were identified by using an early region-specific probe DNA labeled with ^{32}P by nick translation. Bands consist of the two mRNAs which encode large and small T antigens. (B) Analysis of large T antigen. Cells were labeled for 1 h with [^{35}S]methionine, and extracts were prepared and subjected to immunoprecipitation with a large T-antigen-specific monoclonal antibody. (C) Analysis of DNA replication. Low-molecular-weight DNA was isolated from infected cells at the indicated times, digested with *Hin*dIII, and subjected to DNA blot analysis. SV40 DNA was labeled with ^{32}P by nick translation and used as probe.

VP1 localization appeared modified in the absence of agnoprotein. Next, we explored the possibility that late polypeptides might be abnormally localized within *pm*1493-infected cells. CV-1P cell monolayers were fixed at various times after infection and analyzed by immunofluorescence by using a monoclonal antibody specific for VP1 (mAB594). The appearance and localization of VP1-specific fluorescence were, indeed, somewhat different in mutant and wild-type virus-infected cells (Fig. 9). In the absence of agnoprotein, there was a 6- to 8-h delay in the onset of relatively intense fluorescence. This delay presumably reflects stability or localization effects on fluorescence since VP1 was synthesized at similar rates in *pm*1493 and *wt*830-infected cells throughout the time course of fluorescent observations (Fig. 7). In addition to the delay, fluorescence in the mutant virus-infected cells tended to be localized to a perinuclear position to a greater degree than in the wild-type virus-infected cells. Both of these conclusions must be qualified. First, although a delay was observed in the vast majority of *pm*1493-infected cells, occasional cells displayed fluorescence just as bright as that observed in similarly staged *wt*830 infections. Second, although perinuclear localization is considerably more pronounced in the mutant, some mutant-infected cells exhibited uniform nuclear fluorescence and individual wild-type cells often displayed perinuclear staining. In fact, perinuclear fluorescence for VP1 in wild-type virus-infected TC7 monkey cells has been well documented by Kasamatsu and Nehorayan (21, 22). Nevertheless, the general trends of delayed onset and then predominantly perinuclear fluorescence in *pm*1493-infected cells were clear. By 48 h, however, fluorescent patterns were very similar in mutant and wild-type infections; both were markedly perinuclear.

Localization of VP1 was further investigated by biochemical fractionation of infected cells. Cells were labeled for either 1 h (Fig. 10A) or 20 h (Fig. 10B) with [^{35}S]methionine and then fractionated into nuclear, outer nuclear membrane, and cytoplasmic fractions. Localization of VP1 was similar for *pm*1493 and *wt*830-infected cells. Under both labeling conditions, the preponderance of VP1 fractionated into the nuclear compartment. Only small quantities were evident in outer nuclear membrane and cytoplasmic compartments. Interestingly, under long-term labeling conditions where labeled VP1 was representative of steady-state levels, we consistently observed a 50% reduction in VP1 accumulation in mutant versus wild-type virus-infected cells (Fig. 10B). Apparently, VP1 is less stable in the absence of agnoprotein, since the rate of VP1 synthesis in mutant and wild-type virus-infected cells is similar (Fig. 7 and 10A).

In sum, the fluorescence and biochemical fractionation data suggest that in the absence of agnoprotein VP1 is localized somewhat differently within the nucleus and the level to which it accumulates is reduced by half.

Virions were released inefficiently from infected cells in the absence of agnoprotein. Altered VP1 localization could have an impact on release of mature virions from infected cells. This would fit nicely with the small plaque size exhibited by agnogene mutants. Inefficient release would have been

TABLE 2. Analysis of late unit transcription rates by nuclear runoff[a]

	No. of cpm upstream	Upstream (cpm/U)	No. of cpm downstream	Downstream (cpm/U)	Upstream/ downstream
*wt*830	2,870	49.5	1,268	3.7	13.5
*pm*1493	2,191	37.1	839	2.4	15.5

[a] Nuclei were prepared at 36 h after infection of CV-1P cells and incubated for 15 min at 30°C in the presence of [^{32}P]UTP. Nuclear RNA was prepared and hybridized to single-stranded probe DNAs that corresponded mainly to the region upstream or downstream of the transcriptional termination or pausing site which is located at sequence position 421. Results were normalized to counts per minute (cpm) hybridized per unit of residue in the probe sequence. A background of 0.1 cpm per unit of residue has been subtracted from all data.

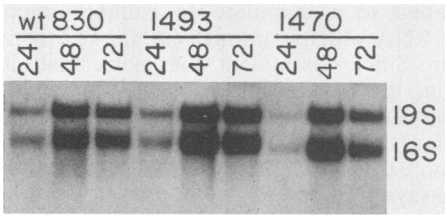

FIG. 5. RNA blot analysis of late mRNAs produced in mutant and wild-type virus-infected cells. CV-1P cells were infected at a multiplicity of 4 PFU per cell, and cytoplasmic, poly(A)$^+$ RNA was prepared at the times indicated above each lane. Late mRNAs were identified by using a late region-specific probe DNA that was labeled with ^{32}P by nick translation. 19S and 16S species are designated.

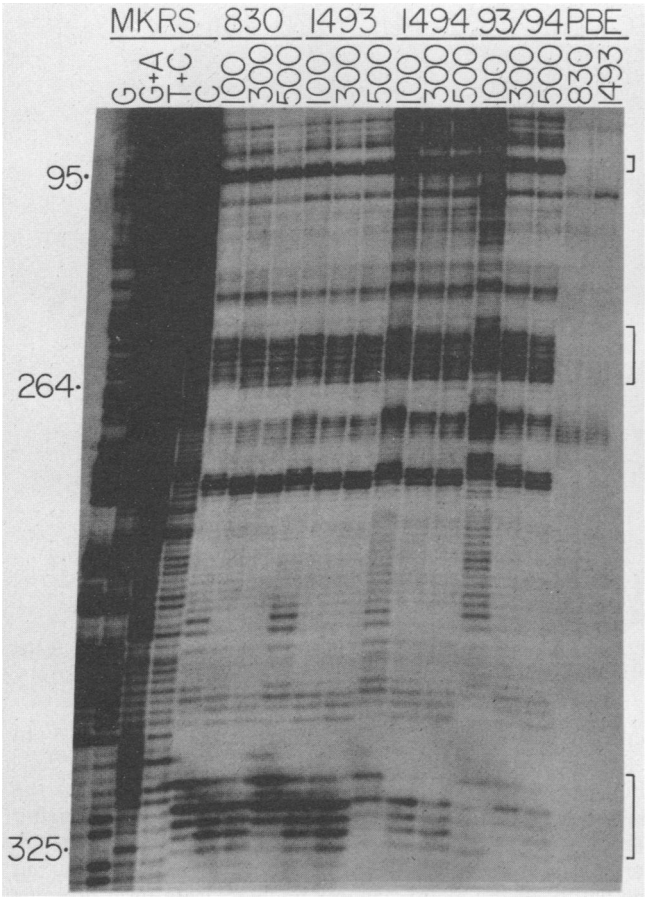

FIG. 6. 5′ S1 endonuclease analysis of late mRNAs produced in mutant and wild-type virus-infected cells. Cytoplasmic, poly(A)$^+$ RNA was prepared at 48 h after infection of CV-1P cells at a multiplicity of 4 PFU per cell. Probe DNAs were 5′ end labeled at sequence position 348 and extended to position 1. Increasing amounts of S1 nuclease were used to digest each hybridized reaction, and the number of units is indicated above each lane. Sequencing ladders are included as markers. The positions of the main 5′ cap sites (sequence positions 325, 264, and 95) were determined from the markers and are indicated. PBE designates reactions which received probe DNA but no mRNA.

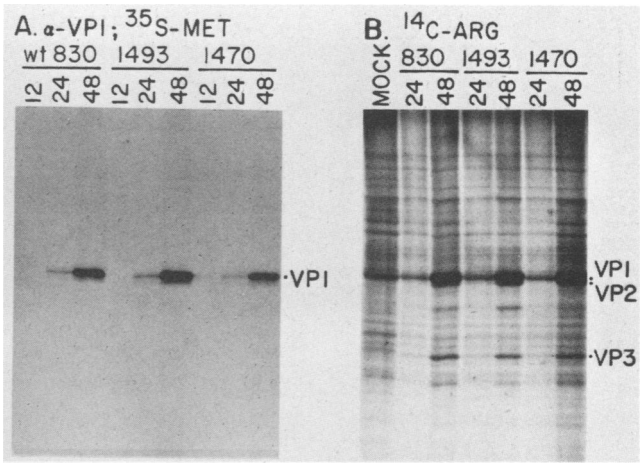

FIG. 7. Analysis of late viral polypeptides synthesized in CV-1P cells after infection with mutant or wild-type viruses. Cells were infected at a multiplicity of 4 PFU per cell and labeled for 1 h with [^{35}S]methionine (A) or for 1.5 h with [^{14}C]arginine (B) at the times indicated above each lane. Extracts were prepared, and [^{35}S]methionine-labeled material was subjected to immunoprecipitation by using a VP1-specific monoclonal antibody, whereas [^{14}C]arginine-labeled extracts were subjected to electrophoresis directly. Bands corresponding to VP1, VP2, and VP3 are designated.

missed in the growth analysis presented in Fig. 3, since cultures (cells plus medium) were subjected to multiple freeze-thaw cycles, a procedure routinely used to mechanically release virus from cells. To test the efficiency of release, infected CV-1P cell cultures were divided into cellular and extracellular (medium) components before freeze-thaw cycles and plaque assay. The result was striking (Fig. 11). Although the intracellular yield of the two viruses never differed by a factor of more than three, the extracellular yield of *pm*1493 compared with that for *wt*830 was reduced by as much as 100-fold at 36 and 42 h after infection. In the absence of agnoprotein, cellular release and, therefore, cell-to-cell spread of SV40 was significantly diminished.

DISCUSSION

Agnoprotein is not required for efficient growth of SV40 in a variety of monkey cell lines. Mutant *pm*1493 contains an A/T to T/A transversion within the translational initiation codon of the agnogene (Fig. 1) and fails to produce agnoprotein (Fig. 2). Nevertheless, it grows to nearly 30% of wild-type yields in CV-1P and AGMK cells and displays no growth defect at all in BSC-1 cells (Fig. 3). Some, but not all, deletion mutations which disrupt the agnoprotein domain have been reported to exhibit somewhat more severe defects (10- to 15-fold [35, 37, 44, 48]). Indeed, the insertion mutant reported here (*in*1494; Fig. 1) exhibited a more severe growth defect (Table 1). We believe the poor growth of *in*1494 is due in part to fusion of an agnoprotein segment to the N terminus of VP2. Presumably, the agnogene deletion

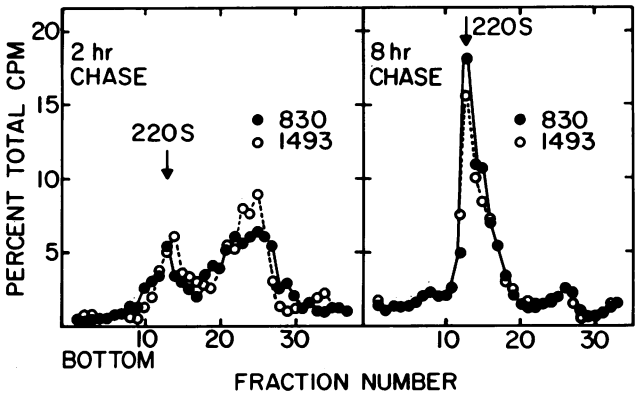

FIG. 8. Velocity sedimentation analysis of virus-specific nucleoproteins synthesized in CV-1P cells after infection with mutant or wild-type viruses. Cells were labeled with [^{3}H]thymidine for 15 min at 36 h after infection at a multiplicity of 4 PFU per cell. After a 2 or 8-h chase, extracts were prepared and nucleoproteins were resolved by velocity sedimentation in sucrose gradients. Gradients were fractionated, and the radioactivity in each fraction was quantitated. The arrow in each panel marks the position of intact, [^{35}S]methionine-labeled virions included as markers.

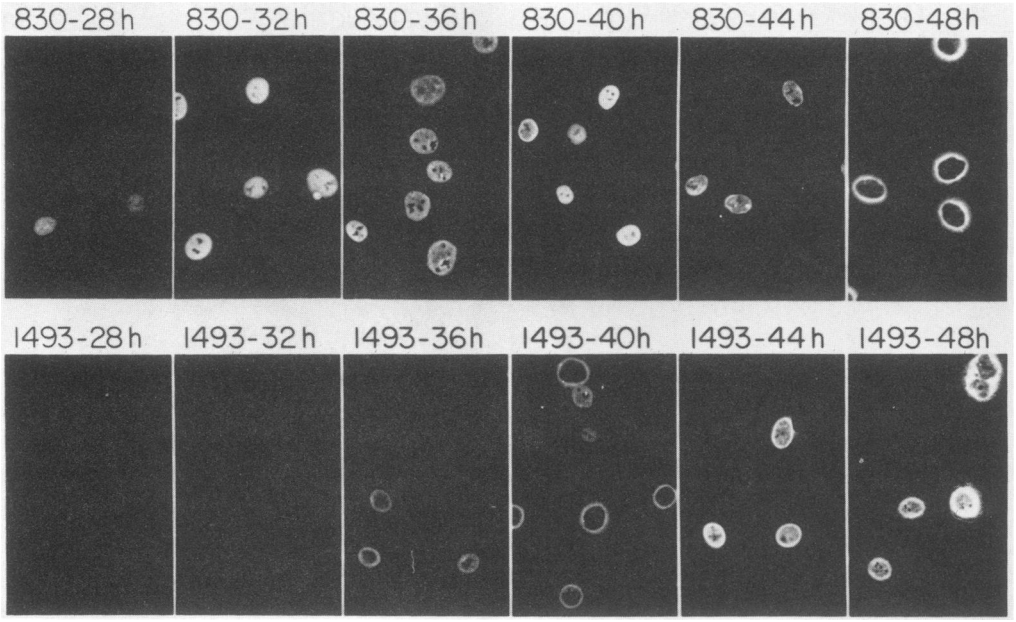

FIG. 9. VP1-specific immunofluorescence of cells infected with *pm*1493 or *wt*830. Immunofluorescence assays were performed at the indicated times after infection of CV-1P cells at a multiplicity of 1 PFU per cell and used a VP1-specific monoclonal antibody.

mutations also generate secondary effects which have an impact on virus growth.

It is difficult to predict the impact of biochemical perturbations on the overall dynamics and yield of a virus infection. Nevertheless, it seemed likely that alterations in the growth cycle of *pm*1493 would prove to be subtle given the modest reduction in final yield we observed for the virus. This proved to be the case. Early-gene expression, DNA replication (Fig. 4), and late transcription rates (Table 2) were all normal in the absence of agnoprotein. Late mRNAs reproducibly accumulated to slightly higher levels (1.5- to 2-fold) in *pm*1493 than they did in *wt*830-infected CV-1P cells (Fig. 5), but the lack of agnoprotein had no effect on the position of late mRNA 5′ ends (Fig. 6). The somewhat higher steady-state levels of late mRNA must be due to a posttranscriptional event since transcription rates were normal, but the nature of the event remains unclear. Late viral proteins were synthesized at normal rates (Fig. 7), but VP1 accumulated to slightly reduced levels in the absence of agnoprotein (Fig. 10B). The twofold effect on steady-state levels of VP1

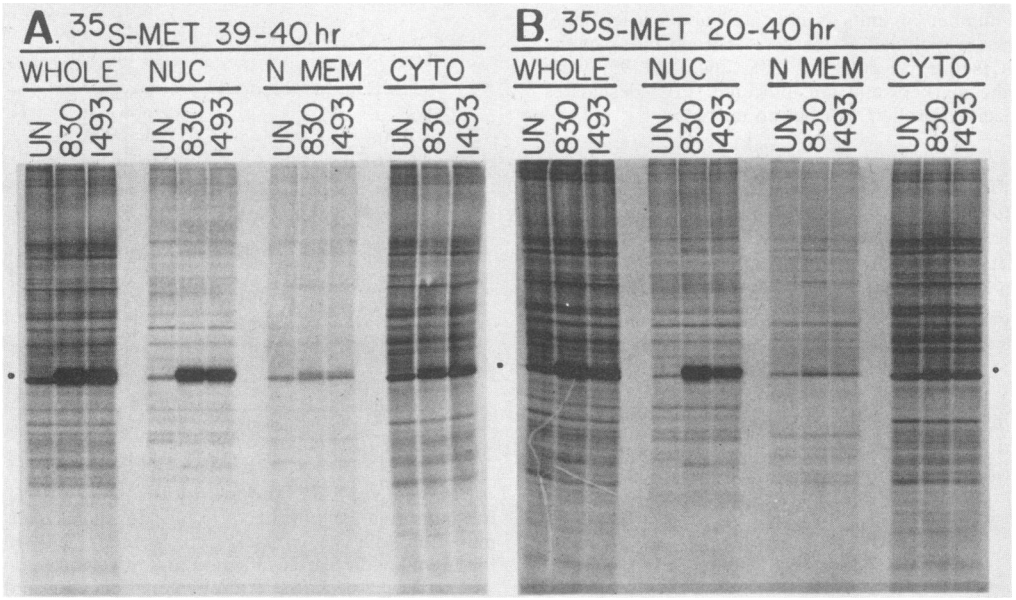

FIG. 10. Analysis of late viral polypeptides synthesized in CV-1P cells after infection with mutant or wild-type viruses. Cells were labeled with [^{35}S]methionine for 1 h (A) or 20 h (B), ending at 40 h after infection at a multiplicity of 4 PFU per cell. Unfractionated extracts (WHOLE) or extracts fractionated into nuclear (NUC), outer nuclear membrane (N MEM), and cytoplasmic (CYTO), components were subjected to electrophoresis. Lanes UN, uninfected. Dots mark bands corresponding to VP1.

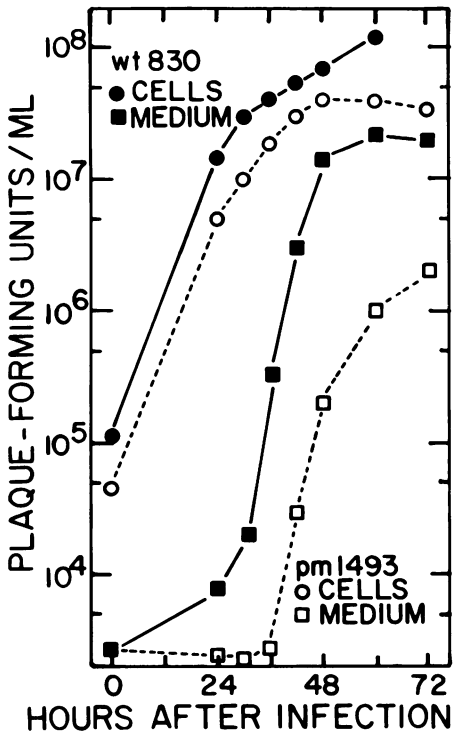

FIG. 11. Kinetics of virus appearance in intracellular and extracellular compartments of infected cultures. CV-1P cells were infected at a multiplicity of 4 PFU per cell. At the indicated times, cells and medium were separated. Cells were suspended in fresh medium, and both components of the original infected culture were subjected to three freeze-thaw cycles. Infectivity was then determined by plaque assay on CV-1P cells.

might result from abnormal localization in *pm*1493-infected cells (discussed below). Finally, we detected no change in the efficiency with which 220S virus particles were assembled in mutant-infected cells (Fig. 8), and mutant, and wild-type virions were equally stable to heat (data not shown).

VP1 proved to be localized somewhat differently in the absence of agnoprotein (Fig. 9). From 28 through 44 h after infection VP1 fluorescence was predominantly perinuclear in *pm*1493-infected cells while *wt*830-infected cultures exhibited more uniform nuclear fluorescence. As mentioned previously, perinuclear fluorescence was readily observed within wild-type infected cell populations, and cells with uniformly staining nuclei could be found among mutant-infected populations. Nevertheless, taken as a whole, the differential staining patterns were convincing. S. Carswell and J. Alwine (personal communication) have noted a similar alteration to VP1 localization in cells infected with agnogene mutants. Biochemical fractionation experiments indicated that the vast majority of VP1 was contained within the nuclear compartment, irrespective of the presence of agnoprotein (Fig. 10). Thus, the perinuclear staining must detect VP1 which remains within the nucleus. Since we do not yet know the specificity of the monoclonal antibody to VP1 it is not possible to say whether our data reflects the location of assembled, intact virions, free VP1, or both.

There is strong genetic evidence that VP1 and the agnoprotein interact. Margolskee and Nathans (28) have reported that pseudorevertants of a VP1 mutant map in the agnogene. Similarly, A. Barkan and J. E. Mertz (A. Barkan, Ph.D. thesis, University of Wisconsin, Madison, 1983) have isolated a phenotypic revertant of an agnogene deletion mutant which carries a second-site mutation in VP1. Thus, it makes sense that VP1 could be localized somewhat differently in the absence of a protein with which it normally interacts.

In addition to the perturbation of VP1 localization, the lack of agnoprotein led to inefficient release of mature virus from the infected cell (Fig. 11). This fits nicely with the fact that agnogene mutants produce quite small plaques (Table 1). The mechanistic basis for the inefficient release is not yet clear. Conceivably, agnoprotein actively participates in the breakdown of infected cells. We favor the hypothesis that agnoprotein influences the localization or intranuclear associations of mature virus particles to favor efficient exit or release of the virus as the infected cell dies. The immunofluorescent data (Fig. 9) may well detect such an influence.

The ability to exit from an infected cell, and, as a result, spread from cell to cell would likely be very important to the virus in its natural host. Agnogene mutants could be severely compromised in their ability to propagate in monkeys.

ACKNOWLEDGMENTS

We thank Ed Harlow and Gilbert Jay for gifts of antibodies to VP1 and agnoprotein, respectively, and Long-Sheng Chang for help with immunofluorescence.

This work was supported by Public Health Service grant CA38965 from the National Cancer Institute. James Resnick was a Postdoctoral Fellow of the Damon Runyon-Walter Winchell Cancer Fund and Thomas Shenk is an American Cancer Society Research Professor.

LITERATURE CITED

1. **Aloni, Y., and N. Hay.** 1985. Attenuation may regulate gene expression in animal viruses and cells. Crit. Rev. Biochem. **18**:327–383.
2. **Alwine, J. C.** 1982. Evidence for simian virus 40 late transcriptional control: mixed infections of wild-type simian virus 40 and a late leader deletion mutant exhibit *trans* effects on late viral RNA synthesis. J. Virol. **42**:798–803.
3. **Alwine, J. C., D. J. Kemp, and G. R. Stark.** 1977. Method for detection of specific RNAs in agarose gels by transfer to diazobenzyloxymethyl-paper and hybridization with DNA probes. Proc. Natl. Acad. Sci. USA **74**:5350–5354.
4. **Buchman, A. R., L. Burnett, and P. Berg.** 1980. The SV40 nucleotide sequence, p. 799–829. *In* J. Tooze (ed.), DNA tumor viruses. Cold Spring Harbor Laboratory, Cold Spring Harbor, N.Y.
5. **Canaani, D., C. Kahana, A. Mukamel, and Y. Groner.** 1979. Sequence heterogeneity at the 5′ termini of late SV40 19S and 16S mRNAs. Proc. Natl. Acad. Sci. USA **76**:3078–3082.
6. **Contreras, R., D. Gheysen, J. Knowland, A. Van de Voorde, and W. Fiers.** 1982. Evidence for the direct involvement of DNA replication origin in synthesis of late SV40 RNA. Nature (London) **300**:500–505.
7. **Dhar, R., K. Subramanian, J. Pan, and S. M. Weissman.** 1977. Structure of a large segment of the genome of simian virus 40 that does not encode known proteins. Proc. Natl. Acad. Sci. USA **74**:827–831.
8. **Fitzgerald, M., and T. Shenk.** 1981. The sequence 5′-AAUAAA-3′ forms part of the recognition site for polyadenylation of late SV40 mRNAs. Cell **24**:251–260.
9. **Ghosh, P. K., M. Piatak, J. E. Mertz, S. M. Weissman, and P. Lebowitz.** 1982. Altered utilization of splice sites and 5′ termini in late RNAs produced by leader region mutants of simian virus 40. J. Virol. **44**:610–624.
10. **Ghosh, P. K., V. B. Reddy, J. Swinscoe, P. V. Choudary, P. Lebowitz, and S. M. Weissman.** 1978. The 5′-terminal leader sequence of late 16S mRNA from cells infected with SV40. J. Biol. Chem. **253**:3643–3647.

11. **Ghosh, P. K., V. B. Reddy, J. Swinscoe, P. Lebowitz, and S. M. Weissman.** 1978. Heterogenicity and 5'-terminal structures of the late RNAs of SV40. J. Mol. Biol. **126**:813–846.
12. **Groudine, M., M. Peretz, and H. Weintraub.** 1981. Transcriptional regulation of hemoglobin switching in chicken embryos. Mol. Cell. Biol. **1**:281–288.
13. **Haegeman, G., H. Van Heuverswyn, D. Gheysen, and W. Fiers.** 1979. Heterogeneity of the 5' terminus of late mRNA induced by a viable simian virus 40 deletion mutant. J. Virol. **31**:484–493.
14. **Harlow, E., L. V. Crawford, D. C. Pim, and N. M. Williamson.** 1981. Monoclonal antibodies specific for the simian virus 40 tumor antigens. J. Virol. **39**:861–869.
15. **Hay, N., and Y. Aloni.** 1985. Attenuation of late simian virus 40 mRNA synthesis is enhanced by the agnoprotein and is temporally regulated in isolated nuclear systems. Mol. Cell. Biol. **5**:1327–1334.
16. **Hay, N., H. Skolnik-David, and Y. Aloni.** 1982. Attenuation in the control of SV40 gene expression. Cell **29**:183–193.
17. **Hirt, B.** 1967. Selective extraction of polyoma DNA from infected mouse cultures. J. Mol. Biol. **26**:365–369.
18. **Hofer, E., and J. E. Darnell.** 1981. The primary transcription unit of the mouse β-major globin gene. Cell **23**:585–593.
19. **Jackson, V., and R. Chalkley.** 1981. Use of whole cell fixation to visualize replicating and maturing simian virus 40: identification of a new viral gene product. Proc. Natl. Acad. Sci. USA **78**:6081–6085.
20. **Jay, G., S. Nomura, C. W. Anderson, and G. Khoury.** 1981. Identification of the SV40 agnogene product: a DNA binding protein. Nature (London) **291**:346–349.
21. **Kasamatsu, H., and A. Nehorayan.** 1979. Intracellular localization of viral polypeptides during simian virus 40 infection. J. Virol. **32**:648–660.
22. **Kasamatsu, H., and A. Nehorayan.** 1979. Vp1 affects intracellular localization of Vp3 polypeptide during SV40 infection. Proc. Natl. Acad. Sci. USA **76**:2808–2812.
23. **Kurilla, M. G., H. Piwnica-Worms, and J. D. Keene.** 1982. Rapid and transient localization of the leader RNA of vesicular stomatitis virus in the nuclei of infected cells. Proc. Natl. Acad. Sci. USA **79**:5240–5244.
24. **Laemmli, U. K.** 1970. Cleavage of structural proteins during the assembly of the head of bacteriophage T4. Nature (London) **227**:680–685.
25. **Lai, C-J., R. Dhar, and G. Khoury.** 1978. Mapping the spliced and unspliced late lytic SV40 RNAs. Cell **14**:971–982.
26. **Laub, O., E. B. Jakobovits, and Y. Aloni.** 1980. 5,6-dichloro-1-β-D-ribofuranosyl-benzimidazole (DRB) enhances premature termination of late SV40 transcription. Proc. Natl. Acad. Sci. USA **77**:3297–3301.
27. **Lebowitz, P., and S. M. Weissman.** 1979. Organization and transcription of the simian virus 40 genome. Curr. Top. Microbiol. Immunol. **87**:43–172.
28. **Margolskee, R. F., and D. Nathans.** 1983. Suppression of a VP1 mutant of simian virus 40 by missense mutations of serine codons of the viral agnogene. J. Virol. **48**:405–409.
29. **Matteucci, M. D., and M. H. Caruthers.** 1981. Synthesis of deoxyoligonucleotides on a polymer support. J. Am. Chem. Soc. **103**:3185–3190.
30. **Maxam, A. M., and W. Gilbert.** 1977. A new method for sequencing DNA. Proc. Natl. Acad. Sci. USA **74**:560–564.
31. **McGrogan, M., D. J. Spector, C. Goldenberg, D. N. Halbert, and H. J. Raskas.** 1979. Purification of specific adenovirus 2 RNAs by preparative hybridization and selective thermal elution. Nucleic Acids Res. **6**:593–608.
32. **McKnight, G. S., and R. D. Palmiter.** 1979. Transcriptional regulation of the ovalbumin and conalbumin genes by steroid hormones in chick oviduct. J. Biol. Chem. **254**:9050–9058.
33. **Mertz, J. E., and P. Berg.** 1974. Viable deletion mutants of simian virus 40: selective isolation by means of a restriction endonuclease from *Hemophilus parainfluenzae*. Proc. Natl. Acad. Sci. USA **71**:4879–4883.
34. **Mertz, J. E., and P. Berg.** 1974. Defective simian virus 40 genomes: isolation and growth of individual clones. Virology **62**:112–124.
35. **Mertz, J. E., A. Murphy, and A. Barkan.** 1983. Mutants deleted in the agnogene of simian virus 40 define a new complementation group. J. Virol. **45**:36–46.
36. **Ng, S.-C., J. E. Mertz, S. Sanden-Will, and M. Bina.** 1985. Simian virus 40 maturation in cells harboring mutants deleted in the agnogene. J. Biol. Chem. **260**:1127–1132.
37. **Nomura, S., G. Jay, and G. Khoury.** 1986. Spontaneous deletion mutants arising from a frameshift insertion in the simian virus 40 agnogene. J. Virol. **58**:165–172.
38. **Nomura, S., G. Khoury, and G. Jay.** 1983. Subcellular localization of the simian virus 40 agnoprotein. J. Virol. **45**:428–433.
39. **Piatak, M., P. K. Ghosh, L. C. Norkin, and S. M. Weissman.** 1983. Sequences locating the 5' ends of the major simian virus 40 late mRNA forms. J. Virol. **48**:503–520.
40. **Piatak, M., K. N. Subrahanian, P. Roy, and S. M. Weissman.** 1981. Late mRNA production by viable SV40 mutants with deletions in the leader region. J. Mol. Biol. **153**:589–618.
41. **Rave, N., R. Crkenjakov, and H. Boedtker.** 1979. Identification of procollagen mRNAs transferred to diazobenzylomethyl paper from formaldehyde agarose gels. Nucleic Acids Res. **6**:3559–3567.
42. **Rigby, P. W. J., M. Dieckmann, C. Rhodes, and P. Berg.** 1977. Labeling DNA to high specific activity *in vitro* by nick translation with DNA polymerase I. J. Mol. Biol. **113**:237–251.
43. **Shapiro, A. L., E. Vinuela, and J. B. Maizel.** 1967. Molecular weight estimation of polypeptide chains by electrophoresis in SDS-polyacrylamide gels. Biochem. Biophys. Res. Commun. **28**:815–820.
44. **Shenk, T. E., J. Carbon, and P. Berg.** 1976. Construction and analysis of viable deletion mutants of simian virus 40. J. Virol. **18**:664–671.
45. **Somasekhar, M. B., and J. E. Mertz.** 1985. Sequences involved in determining the locations of the 5' ends of the late mRNAs of simian virus 40. J. Virol. **56**:1002–1013.
46. **Somasekhar, M. B., and J. E. Mertz.** 1985. Exon mutations that affect the choice of splice sites used in processing the SV40 late transcripts. Nucleic Acids Res. **13**:5591–5608.
47. **Southern, E. M.** 1975. Detection of specific sequences among DNA fragments separated by gel electrophoresis. J. Mol. Biol. **98**:503–517.
48. **Subramanian, K. N.** 1979. Segments of simian virus 40 DNA spanning most of the leader sequence of the major late viral mRNA are dispensable. Proc. Natl. Acad. Sci. USA **76**:2556–2560.
49. **Szalay, A. A., K. Grohmann, and R. L. Sinsheimer.** 1977. Separation of complementary strands of DNA fragments on polyacrylamide gels. Nucleic Acids Res. **4**:1569–1578.
50. **Takemoto, K. K., R. L. Kirchstein, and K. Habel.** 1966. Mutants of simian virus 40 differing in plaque size, oncogenicity, and heat sensitivity. J. Bacteriol. **92**:990–994.
51. **Tegtmeyer, P., K. Rundell, and J. K. Collins.** 1977. Modification of simian virus 40 protein A. J. Virol. **21**:647–657.
52. **Villarreal, L. P., R. T. White, and P. Berg.** 1979. Mutational alterations within the simian virus 40 leader segment generate altered 16S and 19S mRNA's. J. Virol. **29**:209–219.
53. **Weaver, R. F., and C. Weissmann.** 1979. Mapping of RNA by a modification of the Berk-Sharp procedure: the 5' termini of 15S β-globin mRNA precursor and mature 10S β-globin mRNA have identical map coordinates. Nucleic Acids Res. **7**:1175–1193.
54. **Weinberg, R. A., and S. Penman.** 1968. Small molecular weight nondisperse nuclear RNA. J. Mol. Biol. **38**:289–304.
55. **Zoller, M. J., and M. Smith.** 1982. Oligonucleotide-directed mutagenesis using M13-derived vectors: an efficient and general procedure for production of point mutations in any fragment of DNA. Nucleic Acids Res. **10**:6487–6500.